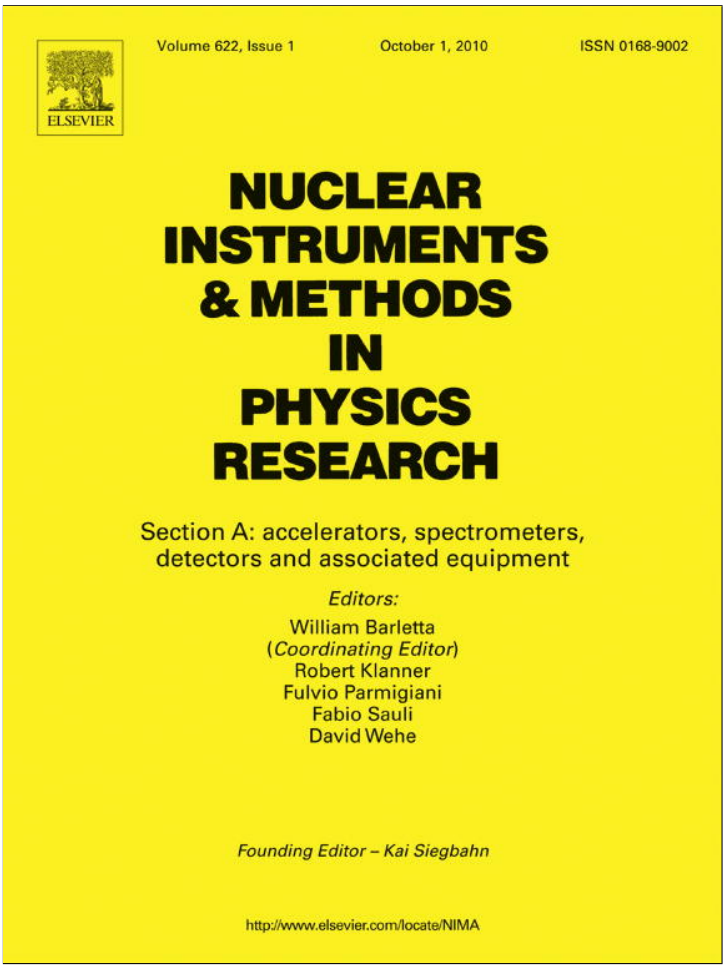

Nuclear Instruments and Methods in Physics Research A 622 (2010) 182–185

Contents lists available at ScienceDirect

Nuclear Instruments and Methods in Physics Research A

journal homepage: www.elsevier.com/locate/nima

Quasi-specular reflection of cold neutrons from nano-dispersed media at above-critical angles

R. Cubitt [a], E.V. Lychagin [b,d], A.Yu. Muzychka [b,d], G.V. Nekhaev [b,d], V.V. Nesvizhevsky [a,d,*], G. Pignol [c], K.V. Protasov [c], A.V. Strelkov [b,d]

[a] Institut Laue-Langevin, 6 rue Jules Horowitz, Grenoble 38042, France
[b] Joint Institute for Nuclear Research, 6 Joliot-Curie, Dubna 141980, Russia
[c] Laboratoire de Physique Subatomique et de Cosmologie, IN2P3/UJF, 53 rue des Martyrs, Grenoble 38026, France
[d] Research Institute of Materials Technology, Presnenskii val 21/18, Moscow 123557, Russia

ARTICLE INFO

Article history:
Received 24 December 2009
Received in revised form
11 June 2010
Accepted 14 July 2010
Available online 21 July 2010

Keywords:
Slow neutrons
Nanodispersed medium
Diamond nanoparticles
Quasi-specular reflection

ABSTRACT

We have predicted and observed for the first time a new phenomenon of quasi-specular reflection of cold neutrons at small incidence angles from nano-dispersed media. this is due to multiple small-angle scattering of neutrons from nano-sized inhomogeneities in the scattering potential. The reflection angle as well as the half-width of angular distribution of diffusively reflected neutrons is approximately equal to the incidence angle. For the powder of diamond nanoparticles used, the reflection probability was equal to ~30% within the detector angular size, which corresponds to 40–50% of total probability (albedo) of quasi-specular reflection. The tangential velocity component of incident neutrons was up to an order of magnitude larger than the critical velocity for pure diamond. We provide an example of potential application of the discovered phenomenon for increasing cold neutron fluxes available for experiments.

1. Introduction

Scattering of waves and particles in disordered media represents an important topic in different domains of science [1]. If scatterers are much larger than radiation wavelength, one deals with small-angle scattering; the average scattering angle is approximately equal to the ratio of the radiation wavelength to the scatterer size. Small-angle scattering, in particular small-angle scattering of cold neutrons including their multiple scattering, represents a powerful method [4–6]. It is applied to study size, geometrical shape, optical potential shape, and relative positions of scattering centers. Multiple scattering of slow neutrons from nanoparticles could be used [7,8] also as a tool in fundamental particle neutron physics [9,10]. Due to multiple small-angle scattering events waves/particles could even reflect from disordered media. Examples are reflection of electromagnetic waves from atmospheric inhomogeneities, aerosols, rain, snow, biological issues, composite materials, etc. [2]. Charged particles (protons, electrons) or neutral particles (atoms) provide another example of wave reflection from disordered media. In the case of small incidence angles one could observe the so-called quasi-specular reflection described in a general form in Ref. [3]. Here, we report the first observation of an analogous phenomenon with slow neutrons.

In the first section we remind the general formalism needed to describe the neutron reflection from powder of nanoparticles. The second section presents the phenomenon of quasi-specular reflection of neutrons from nano-dispersed media. The experimental results are discussed in the third section, and a possible application of this phenomenon is discussed in the fourth section.

2. Formalism

The amplitude of neutron scattering on a round uniform particle in the first Born approximation equals

$$f(\theta) = -\frac{2mU_0}{\hbar^2} r^3 \left(\frac{\sin(qr)}{(qr)^3} - \frac{\cos(qr)}{(qr)^2} \right), \quad q = 2k \sin\left(\frac{\theta}{2}\right) \tag{1}$$

where θ is the scattering angle, m the neutron mass, U_0 the real part of the nanoparticle optical potential [11], $\hbar$ the Planck constant, r the nanoparticle radius, $k = 2\pi/\lambda$ the neutron wave vector, and λ the neutron wavelength. The scattering cross-section equals

$$\sigma_s = \int |f|^2 \, d\Omega = 2\pi \left| \frac{2m}{\hbar^2} U_0 \right|^2 r^6 \frac{1}{4(kr)^2} \left(1 - \frac{1}{(kr)^2} + \frac{\sin(2kr)}{(kr)^3} - \frac{\sin^2(kr)}{(kr)^4} \right). \tag{2}$$

* Corresponding author at: Institut Laue-Langevin, 6 rue Jules Horowitz, Grenoble 38042, France. Tel.: 33 476207795; fax: 33 476207777.
E-mail address: nesvizhevsky@ill.eu (V.V. Nesvizhevsky).

0168-9002/$ - see front matter © 2010 Elsevier B.V. All rights reserved.
doi:10.1016/j.nima.2010.07.049

Consider an idealized case of reflection of a neutron from an infinitely thick loss-free powder of nanoparticles occupying half-space. After multiple scattering events the neutron returns to surface. In the case of non-zero imaginary part of the neutron–nuclei optical potential U_1, finite absorption in nanoparticles with the cross-section

$$\sigma_a = \frac{4\pi}{3}\frac{2m}{\hbar^2}U_1 r^4 \frac{1}{kr} \tag{3}$$

decreases reflectivity. Nevertheless, neutrons with some wave vector are efficiently reflected. Such an albedo of very cold neutrons (VCN) from powder of diamond nanoparticles [12,13] has been measured [14,15], providing the best available reflector in a broad energy range. In particular, neutrons with a wavelength of $\lambda > 2$ nm almost totally reflect from powder of diamond nanoparticles with the average radius of $r \sim 2$ nm at any incident angle. Diamond nanoparticles are chosen for the exceptionally large optical potential of diamond as well as for their availability in nearly optimum sizes. The optimum ratio between the neutron wavelength to the nanoparticle size is $\lambda \sim r$ here; then the scattering angle and the cross-section are large (see Eqs. (1) and (2)).

3. Quasi-specular reflection of neutrons

Now consider faster neutrons so that $\lambda \ll r$ and their absorption in nanoparticles is finite. If so, the angle of neutron scattering on each nanoparticle is small (see Eq. (1)). Therefore neutrons arriving at a large incidence angle penetrate too deep into the powder and they do not return to the surface before they are absorbed. Neutrons arriving at a small incidence angle α could return to surface after multiple small-angle scattering events. Such neutron albedo is analogous to the process considered in a general form in Ref. [3], where an analytical expression describing the angular spectrum of reflected radiation is found for various laws of single scattering of ions, electrons, protons, and photons from a medium consisting of scattering centers with sizes significantly larger than the radiation wavelength. As the typical number of scattering events is small, the exit angle β is not much larger than α, see Fig. 1. In addition, the penetration depth and the path of neutrons in the powder are small; therefore, the absorption affects reflectivity much less than that in Refs. [14,15].

In fact, for the problem parameters used in the present study, the most probable exit angle β is approximately equal to the incidence angle α, with a diffusive halo around this angle. We call such a process quasi-specular reflection of neutrons. Note that coherent scattering of neutrons from neighbouring nanoparticles is neglected here as it is small for the considered case $\lambda \ll r$. Besides, we neglected Mie scattering of neutrons (analyzed for the first time for light scattering on spheres with sizes larger than the light wavelength in Ref. [16]). Mie scattering of neutrons on a single nanoparticle (analogous to Ref. [17]), in contrast with that in the first Born approximation, assumes deviation of some neutrons to very large angles. Our simplification is justified as far as we are interested in the dominant small angle scattering.

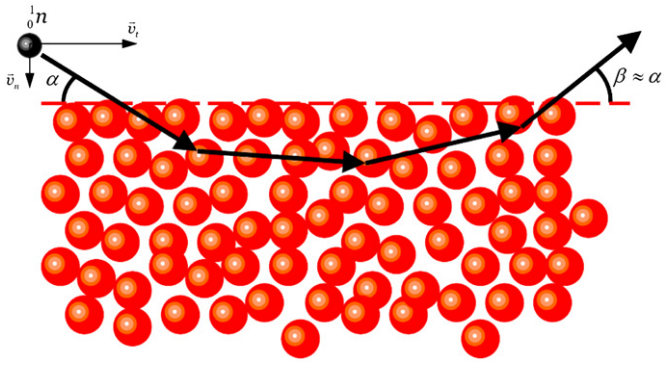

Fig. 1. Sketch of quasi-specular reflection of a cold neutron from powder of nanoparticles.

4. Experiment

The measurements were carried out using a D17 reflectometer [18] at Institut Laue-Langevin, Grenoble. The measuring scheme (top view) is shown in Fig. 2. The neutron beam was shaped using two diaphragms. The height and width of the second diaphragm were equal to 15 and 0.3 mm, respectively, defining the beam size at the sample. The first diaphragm defined an angular divergence of the beam of 0.0004 rad in the horizontal plane. The chopper provided the time-of-flight neutron spectrum measurements to establish the wavelength. Reflected neutrons were counted in a position-sensitive rectangular neutron detector with a height and width of 50 and 25 cm, respectively. The spatial resolution in height and width was equal to 3 and 2.3 mm, respectively. The distance between the sample center and the detector was equal 110 cm. The sample was a powder of diamond nanoparticles with a density of ~ 0.4 g/cm^3 placed into a prism-shape container with a height of 5 cm, a length of ~ 15 cm, and a depth of 4 cm. As nanoparticles in such powders are not available in arbitrary sizes, we could study the size dependence of the neutron reflection from powders only numerically; on the other hand it was easy to perform measurements at different temperatures. The sample was inserted into a special cryostat. The surface of the powder on the neutron beam side was covered with an Al foil of thickness 100 μm. Short vertical sides of the prism were covered with Cd plates with a thickness of 0.5 mm. The cryostat allowed for annealing the sample in vacuum at a temperature of 200 °C, or cooling it down to liquid nitrogen temperature. The sample temperature was measured using a thermo-couple in the middle of the sample. Ballast helium fills in the cryostat and sample for providing thermo-conductivity; thus the sample cooling takes 2 h. Neutron scattering from the cryostat window walls was negligible compared with scattering from the sample.

We studied the angular dependence of neutron reflection probability as a function of neutron wavelength (2–30 Å) and incidence angle (2°, 3°, and 4°). The incidence angle α' equals zero when neutron beam was parallel to the sample surface; the vertical rotation axis of the sample table crosses the sample center. The spectrum and flux of incident neutrons were measured with the sample shifted horizontally by ~ 1 cm out of the beam, the detector was rotated to an angle $2\alpha = 0°$ and shifted horizontally by ~ 1.5 cm. In the scattering measurements, the sample was rotated by an angle α and the detector was rotated by an angle 2α. For each incidence angle α, the sample was shifted horizontally perpendicular to the beam axis in order to maximize

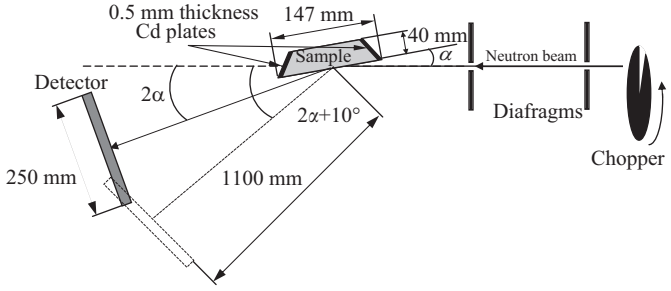

Fig. 2. Scheme of the experiment (top view).

the flux of neutrons scattered to the detector (this translation was equal to 0.0, 0.5, and1.0 mm, respectively). For each grazing angle α, the detector was rotated also to an angle $2\alpha+10^\circ$. Thus, we measured two-dimensional distributions of scattered neutrons within the azimuth angle of 24° and the polar angle range between 0° and $\sim\alpha+15^\circ$.

All measurements were carried out twice: (1) at ambient temperature, after preceding sample treatment (long annealing and heating at 150 °C) and (2) at liquid nitrogen temperature. The total measuring time was 14 h.

Fig. 3 shows the probability of neutron reflection within the detector solid angle as a function of neutron wavelength and incidence angle (as defined in Fig. 2). The reflectivity values in Fig. 3 are smaller than the actual ones by a fraction of neutrons scattered to angles larger than the detector solid angle. Results of measurements at ambient and nitrogen temperature do not differ significantly. In particular, this is due to the small number of scattering events involved in quasi-specular reflection. Besides, the temperature-dependent inelastic neutron scattering is small ($\sigma_{in}(2200\,m/s)=1\,b$) compared with temperature-dependent elastic cross-section ($\sigma_{el}=120\,b$), and the fraction of hydrogen atoms in annealed nanoparticles is low: 1/15. Moreover, hydrogen is strongly bound to carbon; the phonon excitation spectrum is close to that for diamond. Any neutron scattering at hydrogen (both elastic and inelastic ones) is isotropic; therefore such a scattered neutron is almost totally lost. We estimate neutron losses at hydrogen to be equal to 20–40% for various incident angles α actually used. The wavelength range of effective quasi-specular reflection is limited to below $\sim$4 Å by the Bragg scattering of neutrons in the bulk of a diamond nanoparticle.

Computer simulation of quasi-specular reflection is straightforward; it is based on formulas (1)–(3). The simulation method has been verified in our preceding works [14,15]; it is useful for understanding general features of the phenomenon. The measurement geometry used here is shown in Fig. 2. The powder density, fraction of hydrogen, and the scattering cross-sections are given above. The measured data are compared to the model for the neutron incidence angle 2° and wavelength $\lambda=10$ Å. Within a simplified hypothesis of equal size distribution of nanoparticles, such an average diameter appeared to be equal to 2 nm. This model was expanded to other values of the neutron incidence angles and wavelengths. The calculated reflection probabilities defined as described above are shown in Fig. 3 with solid lines.

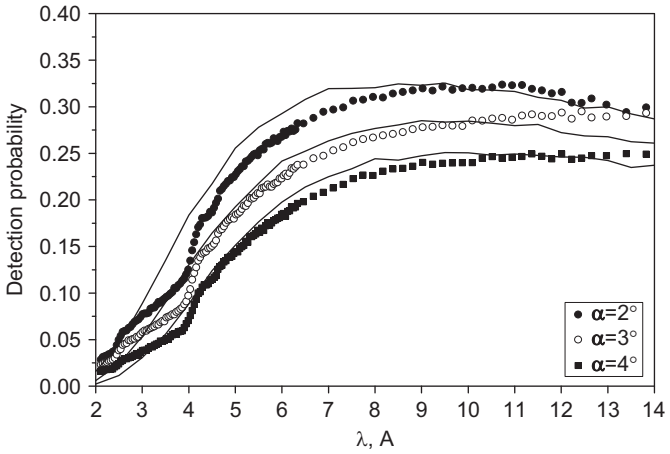

Fig. 3. Probability of neutron reflection within the detector solid angle is shown as a function of neutron wavelength. The incidence angle α is equal to 2°, 3°, and 4°. Dark and empty circles as well as squares correspond to measured data; solid lines illustrate calculations.

4.1. *Dark and empty circles correspond to measured data and solid lines illustrate calculations*

Fig. 4 shows measured (dark and empty circles) and calculated (solid lines) angular distributions of reflected neutrons; the neutron incidence angle is 2°. The data are averaged over two ranges of wavelengths of incident neutrons: 4–5, and 8–9 Å. The neutron count rates in the position-sensitive detector for every deviation angle are divided by the incident neutron flux at the same wavelengths. Analogous wavelength and angular distributions were measured for incidence angles 3° and 4°. Fig. 4 indicates that some neutrons reach the detector at scattering angles smaller than 0° that contradicts the geometrical constraint shown in Fig. 2. This is probably due to some bloating of the sample during its annealing; the surface is deflected by $\sim$2 mm. However, we will ignore here this correction as we are interested in the observation of a new physical phenomenon and in the investigations of its general features rather than in its precision analysis at this stage of our research. The angular distributions of reflected neutrons are calculated within the model described above. Some broadening of the calculated angular distributions compared to the measured data is explained by the simplification of the model (equal sizes of nanoparticles). Nevertheless, the general agreement of the data and such a simple model is quite good.

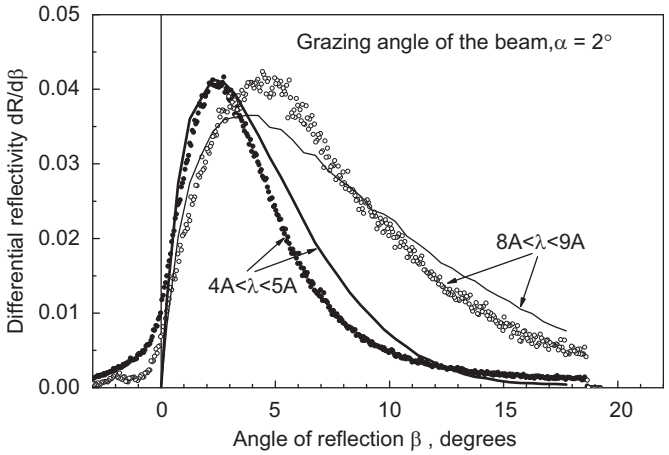

Fig. 4. Angular distributions of reflected neutrons. The incidence angle is equal 2°.

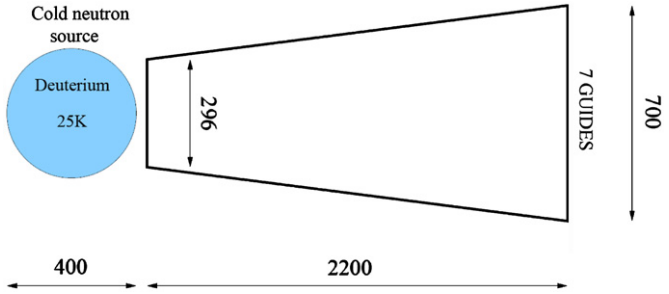

Fig. 5. Geometry of a set of seven neutron guides looking to the cold source at the ILL high-flux reactor (top view). Entrances of the neutron guides are separated from the cold neutron source by a distance of 2.2 m. The width of the assembly of seven neutron guides at this point equals 700 mm; its height equals 200 mm. The effective critical velocity of the neutron guide walls equals 15 m/s ($m=2$ super-mirrors). High radiation fluxes close to the reactor core do not allow installing of super-mirror neutron guides in the mentioned upstream section with the length of 2.2 m.

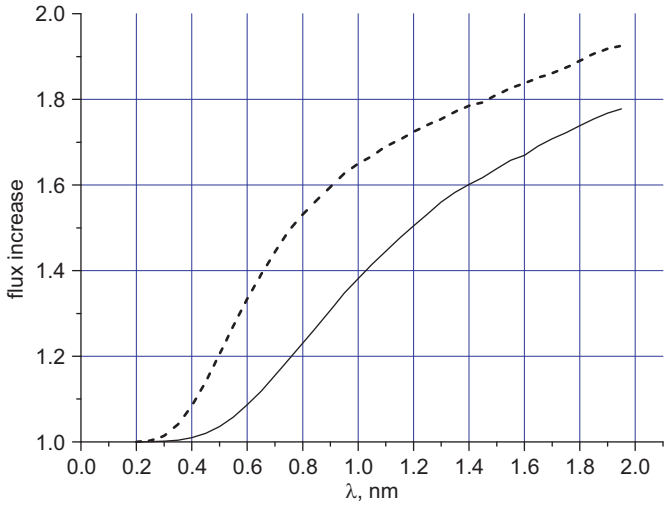

Fig. 6. Increase in the neutron flux at the neutron guide entrance is calculated as a function of neutron wavelength for a reflector made of diamond nanoparticle powder; the reflector geometry is shown in Fig. 5. The solid line corresponds to calculations using nanoparticle powder used in our experiments (hydrogen contamination and nanoparticle sizes are estimated above). The dashed line indicates predictions for "ideal" hydrogen-free powder with the nanoparticle size of 4 nm.

5. Possible application

As we have shown, the quasi-specular reflection of cold neutrons from powder of nanoparticles assumes rather large scattering angles along surface and moderate reflection probability per reflection. Thus one could efficiently profit from this phenomenon only if the number of quasi-specular reflections is limited to a few events and also if rather large resulting angles along the surface are allowed. Therefore the optimal geometry is a slit between two layers of nanoparticle powder, the ratio of the slit length to slit height should not much exceed the mean angle of quasi-specular reflection. Consider, for instance, a set of seven neutron guides looking to the cold neutron source at the high-flux ILL reactor; simplified geometry of this system is shown in Fig. 5.

Using the model and its parameters given above (a powder density of 0.4 g/sm^3, a nanoparticle size of 2 nm, and an absorption length of 64 mm), we calculated the increase in neutron flux at the neutron guides entrance. Only "useful" neutrons with radial velocity of <15 m/s are taken into account. The powder thickness is 4 cm; the shape of the prism formed by the nanoparticle layers is shown in Fig. 5. The results of calculation are presented in Fig. 6.

The calculations showed that the maximum reflectivity is achieved for the nanoparticle size of about 4 nm. This result is compared in Fig. 6 to the calculations carried out for the actually used powder. In order to access the feasibility of using diamond nanoparticles in the highest radiation fluxes, we plan to carry out a dedicated study.

6. Conclusion

We predicted and observed for the first time the phenomenon of quasi-specular reflection of cold neutrons from flat surface of nano-dispersed medium at small incidence angles. It occurs due to multiple small-angle scattering of neutrons on nano-sized inhomogeneity of the optical neutron–nuclei potential. In contrast with standard sub-critical reflection of neutrons from optical potential of uniform medium, the quasi-specular reflection might be observed also at highly above-critical angles. Moreover, powders of diamond nanoparticles used here reflect neutrons with perpendicular velocity components larger than 40 m/s, the cut-off for the best super-mirrors available [19]. The wavelength range of effective quasi-specular reflection is limited from below to $\sim$4 A by the Bragg scattering in diamond. We provide an example of potential application of the discovered phenomenon for increasing cold neutron fluxes available for experiments.

References:

[1] P. Sheng, Scattering and Localization of Classical Waves in Random Media, World Scientific, Singapore, 1990.
[2] A. Ishimaru, Wave Propagation and Scattering in Random Media, John Wiley & Sons Inc., 1999.
[3] V.S. Remizovich, Sov. Phys. JETP. 60 (2) (1984) 290.
[4] J. Schelten, W. Schmatz, J. Appl. Crystallogr. 13 (1980) 385.
[5] L.A. Feigin, D.I. Svergun, in: Structure Analysis by Small-Angle X-ray and Neutron Scattering, Plenum Press, 1987.
[6] T.M. Sabine, W.K. Bertram, Acta Crystallogr. A 55 (1999) 500.
[7] V.V. Nesvizhevsky, Phys. At. Nucl. 65 (3) (2002) 400.
[8] V.A. Artemiev, Atom. Energy 101 (2006) 901.
[9] J.S. Nico, W.M. Snow, Annu. Rev. Nucl. Part. Sci 55 (2005) 27.
[10] H. Abele, Prog. Part. Nucl. Phys. 60 (2008) 1.
[11] E. Fermi, L. Marshall, Phys. Rev. 71 (1947) 666.
[12] P.J. de Carli, J.C. Jameieson, Science 133 (1821) 1961.
[13] A.E. Aleksenskii, M.V. Baidakova, A.Y. Vul, V.I. Siklitskii, Phys. Solid State 41 (1999) 668.
[14] V.V. Nesvizhevsky, E.V. Lychagin, A.Yu. Muzychka, A.V. Strelkov, G. Pignol, K.V. Protasov, Nucl. Instr. and Meth. A. 595 (3) (2008) 631.
[15] E.V. Lychagin, A.Yu. Muzychka, V.V. Nesvizhevsky, G. Pignol, K.V. Protasov, A.V. Strelkov, Phys. Lett. B. 679 (186) (2009).
[16] G. Mie, Annal. Phys. 25 (1908) 377.
[17] V.V. Nesvizhevsky, A.Yu. Voronin, R. Cubitt, K.V. Protasov, Nat. Phys. 6 (2010) 114.
[18] R. Cubitt, G. Fragneto, Appl. Phys. A. 74 (2002) S329.
19 R. Maruyama, et al., Thin Solid Films 515 (2007) 5704.